

Optimizing CIGS Solar Cell Performance: The Impact of Counter Electrode on Electrodeposition Methods

Hilda Rahmawati^{1*}, Nurmalasari Ismail²

¹ Physics Department, Faculty of Science Cokroaminoto Palopo University, Indonesia

² Chemistry department, Faculty of Science Cokroaminoto Palopo University, Indonesia

Corresponding Authors E-mail: hildarmwt@gmail.com

Article Info

Article info:

Received: 10-01-2024

Revised: 22-04-2024

Accepted: 24-04-2024

Keywords:

Solar Cells; CIGS;
Electrodeposition; Counter
Electrode.

How To Cite:

Rahmawati, H., Ismail, N.
(2024). Optimizing CIGS
Solar Cell Performance:
The Impact of Counter
Electrode on
Electrodeposition Methods.
Indonesian Physical
Review, 7 (2) 259-267

DOI:

<https://doi.org/10.29303/ipr.v7i2.301>

Abstract

Copper Indium Gallium Selenium (CIGS) is a type of solar cell with great potential to be developed to meet increasing energy needs. Electrodeposition is the preferred technique for fabricating CIGS solar cells because it is simple, does not require vacuum equipment, and is low-cost. One factor influencing electrodeposition is the counter electrode, so in this research, CIGS will be fabricated using platinum wire and platinum plate as the counter electrode. Based on the XRD results of CIGS oriented at (112), (211), (220), and (312), the UV-Vis results show that the resulting CIGS has an absorbance peak of 390 nm. CIGS solar cell performance results based on photoresponse produce 0.99 s and 0.45 s when using platinum wire and plate consecutively. Both platinum wire and plate as counter electrodes in electrodeposition can produce CIGS solar cells. However, CIGS with a platinum plate as a counter electrode produces more optimal CIGS performance.

Copyright © 2024 Authors. All rights reserved.

Introduction

CIGS solar cells consist of a mixture of copper, indium, gallium, and selenium materials, with a band gap of 1.04 to 3.50 eV [1]. CIGS has high radiation resistance, which can be used as an absorber layer in solar cells [2]. Various methods have been developed to fabricate CIGS solar cells, such as co-evaporating [3], sputtering [4], and heating up [5], but this technique requires vacuum conditions, and production costs are very high. Otherwise, there are non-vacuum methods such as electrodeposition [6], spin coating [7], and spray coating [8]. Electrodeposition is the most preferred method because it is simple, stable, low cost, does not require vacuum conditions, and has been proven capable of producing CIGS solar cells [9].

The author's research group has developed the synthesis of CIGS solutions using the hot injection method and deposited them using knife coating, spin coating, and selenation methods [2], [7], [8].

The deposition results using these three methods are less homogeneous, too thick, and have unstable outputs. So, CIGS synthesis and deposition are carried out using the electrodeposition method to obtain CIGS solar cells with homogeneous and stable output.

Electrodeposition or electrolytic deposition is the conventional process of coating a thin layer of a metal over a different metal to change its surface properties. Electrodeposition works based on the principle of electrolysis, namely using an electric current to reduce the cations of the desired material from the electrolyte and coating the material as a thin layer onto the surface of a conductive substrate [10], [11]. In previous research, CIGS only focused on the materials used [12], [13] and variations in the potential input applied [14]. In contrast, one crucial factor that influences the performance of the electrodeposition process is the counter electrode because the counter electrode plays a role in completing the circuit and ensuring the charge flows [10], [15].

Therefore, in this research, the CIGS electrodeposition process will be carried out using two types of counter electrodes, namely platinum wire and platinum plate, to produce CIGS solar cells with optimal performance. Based on the results obtained, the resulting CIGS performance is optimal, namely 0.45 s when responding to light.

Experimental Method

Sample Preparations

Electrodeposition is carried out using two electrodes, the working and the counter electrodes. In this research, ITO (Indium Tin Oxide) was used as the working electrode, and platinum wire and plate were used as counter electrodes. Start by making a CIGS solution as in the paper [16]. The CIGS materials used in this research are copper (II) acetylacetonate ($\text{Cu}(\text{acac})_2$) Merck, indium (III) chloride (InCl_3) Merck, gallium (III) acetylacetonate ($\text{Ga}(\text{acac})_3$) Merck and selenium dioxide (SeO_2) which was synthesized based on previous research [17]. After that, the resulting CIGS solution is electrodeposited at a voltage of -1.5 V using platinum wire and plate as counter electrodes alternately. The resulting ITO/CIGS thin film was then annealed at 400°C for 60 minutes in a furnace. This process is shown in Figure 1. The resulting samples CIGS will be tested and characterized using several instruments. The structural properties of sample CIGS were characterized using Shimadzu 7000 X-Ray Diffraction (XRD), The optical properties were characterized using UV-Vis Spectrophotometry (Analytik Jena Specord 200 Plus), Morphology sample was characterized using Scanning Electron Microscopy (SEM) FEI type Inspect-S50. After that, the sample was tested using a Keithley 2400 electrometer to determine the performance of the CIGS sample.

Result and Discussion

The resulting CIGS solar cell samples were then characterized using X-ray diffraction (XRD) to identify the diffraction patterns formed. Two samples were obtained: CIGS, which used platinum wire and platinum plate as counter electrodes. The diffraction patterns of the two samples are shown in Figure 2.

Figure 2 (a) shows the CIGS diffraction pattern with platinum wire as a counter electrode, which forms one CIGS diffraction peak, namely at $2\theta = 26.73^\circ$ with plane orientation (112) and one ITO peak, which is the working electrode or substrate used to coat CIGS. Figure 2 (b) shows the CIGS diffraction pattern with a platinum plate as a counter electrode, which then forms CIGS diffraction peaks at $2\theta = 26.65^\circ$, 35.11° , 44.31° and 51.53° with plane orientations, respectively (112), (211), (220), and (312). Based on Mankoshi et al. [18], several peaks of CIGS were found at

$2\theta=26.91^\circ, 28.02^\circ, 35.48^\circ, 42.43^\circ$ until 71.69° , it shows that the peak that appears in the sample indicates that same several previous studies.

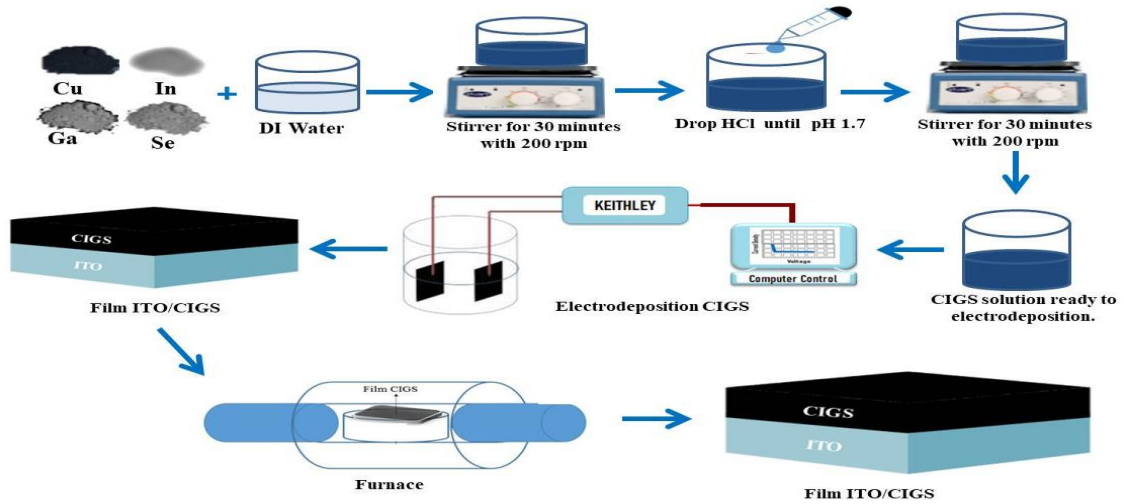


Figure 1. CIGS Solar Cell Fabrication

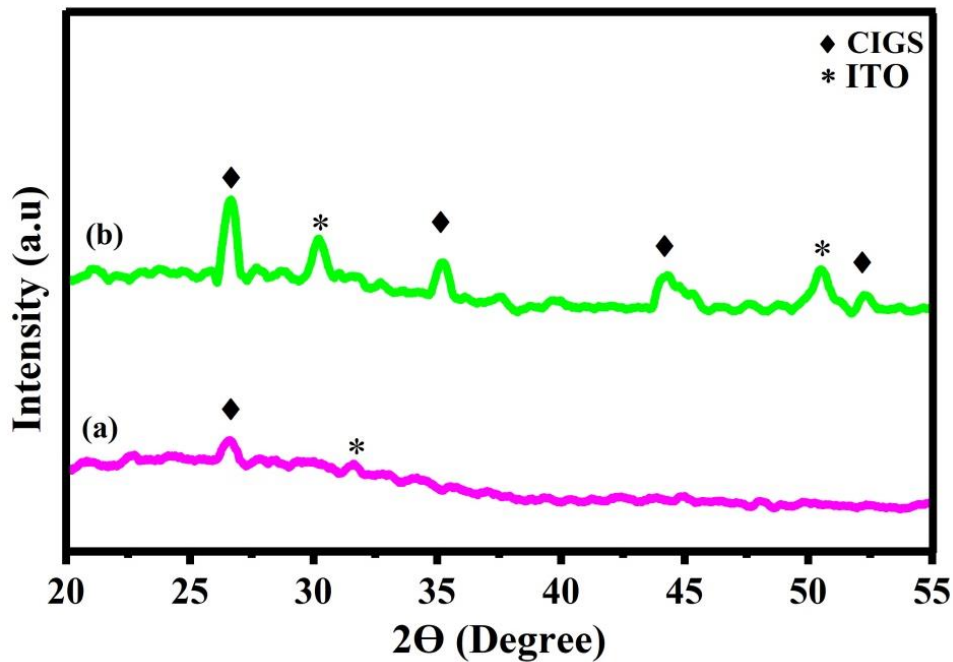


Figure 2. Diffraction pattern of CIGS solar cells (a) Platinum wire (b) Platinum plate

However, platinum is used as a counter electrode because of its inert nature [19], which allows charge to flow during the electrodeposition process. Platinum wire and plates have been shown to produce CIGS diffraction patterns. More CIGS diffraction patterns appear when using a platinum plate as a counter electrode because its size is larger than the working electrode so that the current limit that appears is minimal or even non-existent so that the electrodeposition process can take place optimally and produce CIGS solar cells with high crystallinity [20], [21].

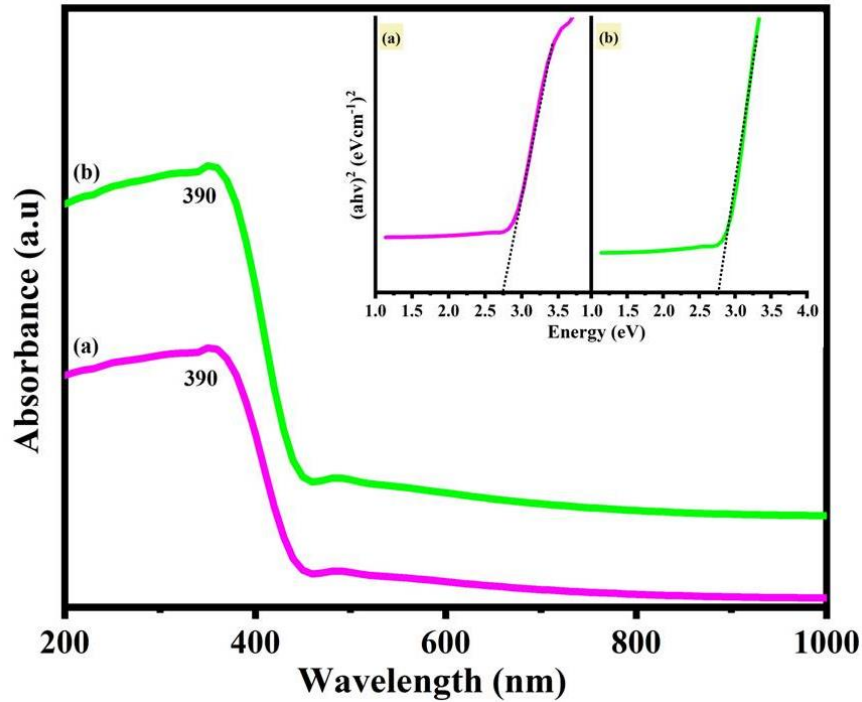


Figure 3. CIGS absorbance spectrum and Tauc plot (a) Platinum wire (b) Platinum plate

Table 1. Peak absorbance and CIGS band gap

Sample	Absorbance (nm)	Band gap (eV)
Platina wire (a)	390	2.75
Platina plate (b)	390	2.75

The absorbance spectrum can be measured using UV-Vis spectroscopy, where there will be an interaction between the sample and light with a wavelength of 200 nm to 900 nm so that UV-Vis spectroscopy can measure the light absorbed by the sample at each wavelength [22], [23]. Figure 3 shows the absorbance spectrum of the resulting CIGS solar cell. For both samples with platinum wire and plate, both absorbance peaks were at 390 nm. Ideally, the CIGS absorbance peak is 380 nm to 1000 nm [1] It can be confirmed that the two CIGS solar cells produced are at the ideal CIGS absorbance peak.

Next, the results of UV-Vis spectroscopic characterization were used to identify the band gap of the CIGS solar cells produced using the Tauc Plot method. The inset in Figure 3 shows the band gap of the resulting CIGS solar cell. The band gap is the minimum energy electrons need to move from the valence band to the conduction band. In the Cu, In, Ga, and Se chalcopyrite alloy system, the band gap varies from 1.04 eV to 3.5 eV [1], [8], [16]. Based on Figure 3 and Table 1, the band gap of CIGS solar cells with platinum wire and plate has an absorbance peak of 390 nm and a band gap of 2.75 eV. These results confirm that both the absorbance and band gap are within the requirements of an ideal CIGS solar cell. At a band gap of 2.75 eV, electron-hole recombination that occurs in the valence and conduction bands can be minimized so that both will produce optimal CIGS solar cell performance.

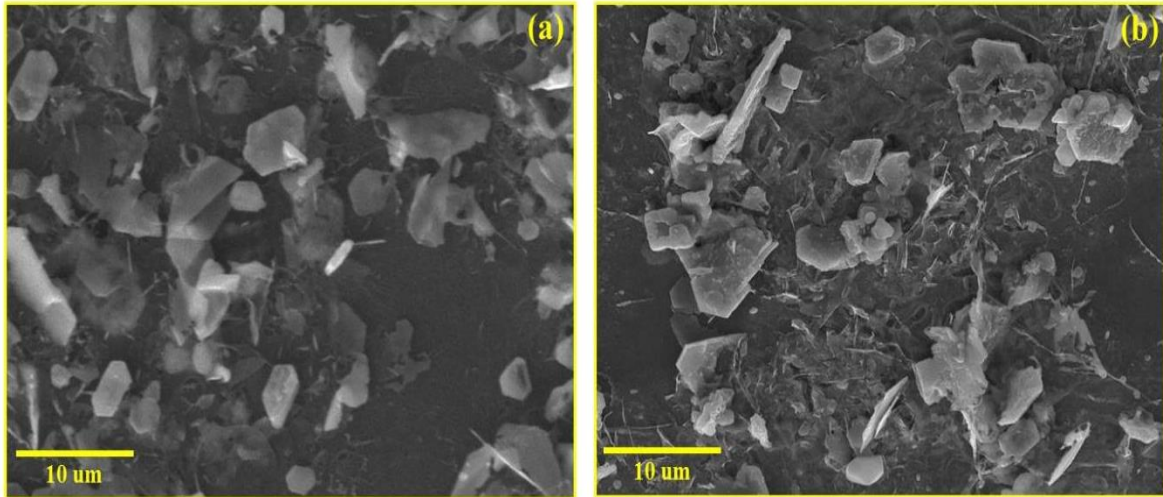


Figure 4. Morphology of CIGS solar cells (a) Platinum wire (b) Platinum plate

Table 2. CIGS film element composition based on EDX characterization.

Sample	Cu (At%)	In (At%)	Ga (At%)	Se (At%)	GGI (Ga/(Ga+In))
Platina wire (a)	26.99	57.01	2.53	13.48	0.05
Platina plate (b)	35.06	14.96	3.76	46.23	0.21

Based on Figure 4 (a and b), the surface of the CIGS solar cells produced tends to be rough and irregular, and the grains formed are also not uniform. The tendency for the sample surface to be rough and have irregular grains is caused by the element being dominated by indium (In) content, which pushes the boundaries between the grains to merge [14], [24]. This is confirmed by Table 2, which shows that the indium (In) content is quite dominant in the CIGS solar cells produced. Even though the surface shape is like that of Figure 4, this does not significantly affect the performance of CIGS solar cells.

The element composition characterized by SEM-EDX is closely related to the intrinsic characteristics of CIGS, such as the GGI ratio ($Ga/(Ga+In)$). The GGI ratio shows the defects formed in CIGS solar cells. If the GGI ratio is 0.3, it can be ascertained that the defects in the solar cells are minimal, thereby facilitating transportation and reducing the recombination process [25]. Based on Table 2, the GGI ratio of CIGS solar cells with platinum plates is closer to 0.3 when compared to CIGS solar cells with platinum wires. So, it can be confirmed that there are fewer defects in CIGS solar cells with platinum plates. It also corresponds to the XRD characterization results where the CIGS peak produced by sample (b) is dominant.

Solar cell performance can be determined by measuring the solar cell's response to light or photoresponse. Photoresponse measurements use the two-probe method that is connected to the electrometer (Keithley 2400), where CIGS film with an area of $1 \times 1 \text{ cm}^2$ will be illuminated with a solar simulator with a power input of 100 mWcm^{-2} for several minutes [26]. Measurements are carried out under an on/off light cycle at specific intervals, as in Figure 5. When the light hits the sample (on), the response current will increase, and when the light is turned off (off), the response current will decrease to the ground state [27].

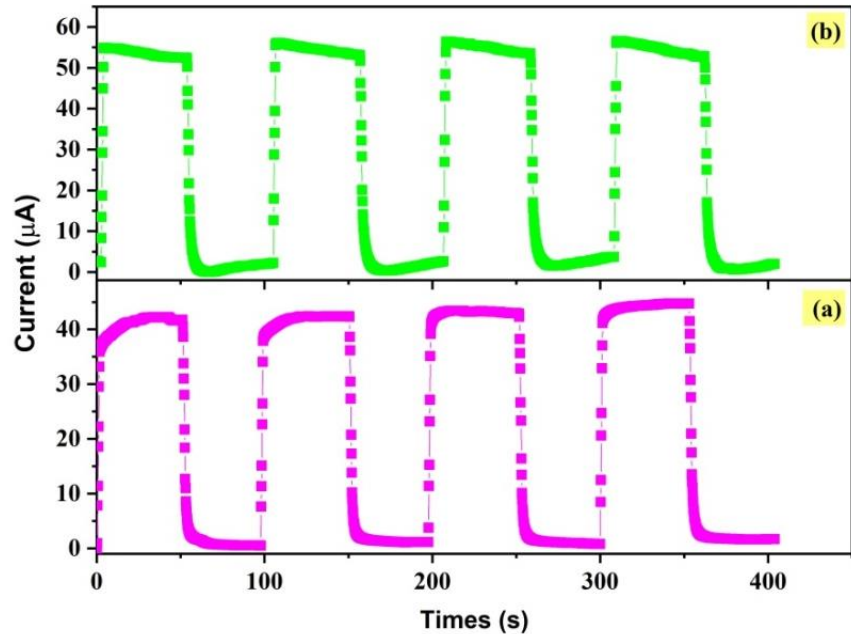


Figure 5. I-t photoresponse of CIGS solar cells (a) Platinum wire (b) Platinum plate

Based on Figure 5, the two samples produced can maintain a stable phase or cycle during measurements. CIGS solar cells (a) achieve a current change of 39.84 μA , and CIGS solar cells (b) achieve a current change of 55.78 μA . High peak current changes are produced due to the lack of electron-hole recombination in the valence and conduction bands, so CIGS solar cells with platinum plates produce higher current changes. It is also confirmed in Table 2, where the GGI ratio of sample (b) is close to 0.3, indicating that the solar cell's defect is minor.

The current and time graphs under the on/off irradiation cycle can be calculated using Eq.

$$I = I_0 + A \exp(-(t - t_0)/\tau) \quad (4.1)$$

Where I is the current as a function of time, t is time, τ is the time required to rise (Light on) or fall (Light off), and A is the amplitude [26].

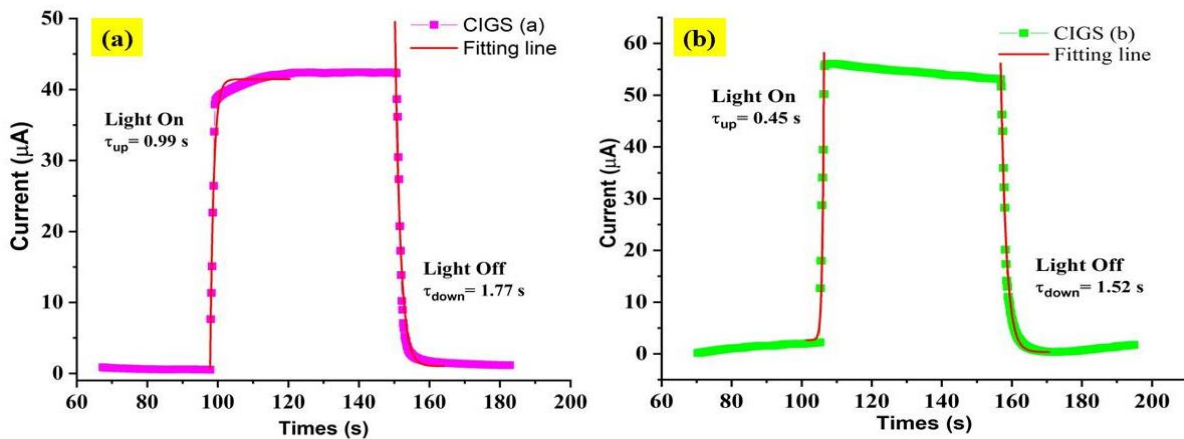


Figure 6. CIGS photoresponse I-t fittings (a) Platinum wire (b) Platinum plate

Table 3. CIGS photoresponse I-t fitting results

Sample CIGS	Light On (τ_{up}) (second)	Light Off (τ_{down}) (second)
Platina wire (a)	0.99	1.77
Platina plate (b)	0.45	1.52

The results of CIGS photoresponse I-t fitting are shown in Figure 6 and Table 3. Based on the results obtained, the time required to respond to light when the light is on is faster than when the light is off; this is due to the large number of trap states that are formed when the light is off, thereby slowing down the movement of the photogeneration carrier [28], [29]. If the solar cell has a response to light of no more than 2 seconds, then it can be said that the solar cell has optimal performance. It can be confirmed that the two samples produced are classified as solar cells with good performance.

Conclusion

CIGS solar cells were electrodeposited in this research using two types of counter electrodes. Based on the results of XRD, UV-Vis, SEM-EDX, and Photoresponse, it can be concluded that this research was successfully carried out. The results show that CIGS solar cells with platinum plates have a light response speed of 0.45 seconds, while those with platinum wires are 0.99 seconds. Based on literature studies, comparisons with previous research, and characterization results, CIGS solar cells with platinum plates as counter electrodes produce CIGS with minimal defects and optimum performance.

Acknowledgment

The authors thank the Universitas Cokroaminoto Palopo (UNCP) for the PDP Internal UNCP research funding with contract number 1586/R/UNCP/XI/2023.

References

- [1] J. Ramanujam and U. P. Singh, "Copper indium gallium selenide based solar cells - A review," *Energy Environ. Sci.*, vol. 10, no. 6, pp. 1306–1319, 2017, doi: 10.1039/c7ee00826k.
- [2] N. Mufti *et al.*, "Review of CIGS-based solar cells manufacturing by structural engineering," *Sol. Energy*, vol. 207, pp. 1146–1157, 2020, doi: 10.1016/j.solener.2020.07.065.
- [3] M. J. Shin *et al.*, "Semi-transparent photovoltaics using ultra-thin Cu(In,Ga)Se₂ absorber layers prepared by single-stage co-evaporation," *Sol. Energy*, vol. 181, pp. 276–284, 2019, doi: 10.1016/j.solener.2019.02.003.
- [4] J. C. Park, M. Al-Jassim, S. W. Shin, J. H. Kim, and T. W. Kim, "Comprehensive characterization of CIGS absorber layers grown by one-step sputtering process," *Ceram. Int.*, vol. 45, no. 4, pp. 4424–4430, 2019, doi: 10.1016/j.ceramint.2018.11.120.
- [5] H. Afshari *et al.*, "The role of metastability and concentration on the performance of CIGS solar cells under Low-Intensity-Low-Temperature conditions," *Sol. Energy Mater. Sol. Cells*, vol. 212, p. 110571, 2020, doi: 10.1016/j.solmat.2020.110571.
- [6] R. L. Oliveri, B. Patella, F. Di Pisa, A. Mangione, G. Aiello, and R. Inguanta, "Fabrication of

- czts/cigs nanowire arrays by one-step electrodeposition for solar-cell application," *Materials (Basel)*, vol. 14, no. 11, p. 2778, 2021, doi: 10.3390/ma14112778.
- [7] A. S. P. Dewi *et al.*, "Synthesis and characterization of CIGS ink by hot injection method," *AIP Conf. Proc.*, vol. 2228, no. April, 2020, doi: 10.1063/5.0000878.
- [8] N. Mufti *et al.*, "Selenization process in simple spray-coated CIGS film," *Ceram. Int.*, vol. 48, no. 15, pp. 21194–21200, 2022, doi: 10.1016/j.ceramint.2022.04.015.
- [9] N. Mufti *et al.*, "Review of CIGS-based solar cells manufacturing by structural engineering," *Sol. Energy*, vol. 207, no. July, pp. 1146–1157, 2020, doi: 10.1016/j.solener.2020.07.065.
- [10] X. Zheng, T. Ahmad, and W. Chen, "Challenges and strategies on Zn electrodeposition for stable Zn-ion batteries," *Energy Storage Mater.*, vol. 39, pp. 365–394, 2021, doi: 10.1016/j.ensm.2021.04.027.
- [11] J. M. Costa and A. F. de Almeida Neto, "Ultrasound-assisted electrodeposition and synthesis of alloys and composite materials: A review," *Ultrason. Sonochem.*, vol. 68, p. 105193, 2020, doi: 10.1016/j.ultsonch.2020.105193.
- [12] R. W. You, K. K. Lew, and Y. P. Fu, "Effect of indium concentration on electrochemical properties of electrode-electrolyte interface of $\text{CuIn}_{1-x}\text{Ga}_x\text{Se}_2$ prepared by electrodeposition," *Mater. Res. Bull.*, vol. 96, pp. 183–187, 2017, doi: 10.1016/j.materresbull.2017.04.027.
- [13] J. Gong *et al.*, "Enhancing photocurrent of $\text{Cu}(\text{In,Ga})\text{Se}_2$ solar cells with actively controlled Ga grading in the absorber layer," *Nano Energy*, vol. 62, pp. 205–211, 2019, doi: 10.1016/j.nanoen.2019.05.052.
- [14] N. D. Sang, P. H. Quang, L. T. Tu, and D. T. B. Hop, "Effect of electrodeposition potential on composition and morphology of CIGS absorber thin film," *Bull. Mater. Sci.*, vol. 36, no. 4, pp. 735–741, 2013, doi: 10.1007/s12034-013-0497-5.
- [15] D. H. Song *et al.*, "Highly porous Ni-P electrode synthesized by an ultrafast electrodeposition process for efficient overall water electrolysis," *J. Mater. Chem. A*, vol. 8, no. 24, pp. 12069–12079, 2020, doi: 10.1039/d0ta03739g.
- [16] H. Rahmawati, M. Tommy Hasan Abadi, S. Zulaikah, and N. Mufti, "Electrodeposition Technique to Fabrication CIGS using Pure Selenium and SeO_2 as Selenium Source," *Malaysian J. Fundam. Appl. Sci.*, vol. 18, no. 3, pp. 367–373, 2022, doi: 10.11113/mjfas.v18n3.2489.
- [17] H. Rahmawati, "Sintesis dan Karakterisasi Selenium menjadi Selenium Dioksida (SeO_2)," *Appl. Phys. Cokroaminoto Palopo*, vol. 4, no. 2, pp. 29–32, 2023, doi: science.e-journal.my.id/apcp/article/view/204.
- [18] M. A. K. Mankoshi, F. I. Mustafa, and N. J. Hintaw, "Effects of Annealing Temperature on Structural and Optical Properties of CIGS Thin Films for Using in Solar Cell Applications," *J. Phys. Conf. Ser.*, vol. 1032, no. 1, 2018, doi: 10.1088/1742-6596/1032/1/012019.
- [19] M. Shoup, A. Ourahmane, E. P. Ginsburg, N. P. Farrell, and M. A. McVoy, "Substitution-inert polynuclear platinum compounds inhibit human cytomegalovirus attachment and

- entry," *Antiviral Res.*, vol. 184, p. 104957, 2020, doi: 10.1016/j.antiviral.2020.104957.
- [20] Y. Xia, D. Nelli, R. Ferrando, J. Yuan, and Z. Y. Li, "Shape control of size-selected naked platinum nanocrystals," *Nat. Commun.*, vol. 12, no. 1, p. 3019, 2021, doi: 10.1038/s41467-021-23305-7.
- [21] K. Jiang *et al.*, "Single platinum atoms embedded in nanoporous cobalt selenide as electrocatalyst for accelerating hydrogen evolution reaction," *Nat. Commun.*, vol. 10, no. 1, p. 1743, 2019, doi: 10.1038/s41467-019-09765-y.
- [22] R. K. Upadhyay and S. Jit, "Solution-processed ZnO nanoparticles (NPs)/CH₃NH₃PbI₃/PTB7/MoO₃/Ag inverted structure based UV-visible-Near Infrared (NIR) broadband photodetector," *Opt. Mater. (Amst.)*, vol. 135, p. 113290, 2023, doi: 10.1016/j.optmat.2022.113290.
- [23] M. B. A. Bashir, A. H. Rajpar, E. Y. Salih, and E. M. Ahmed, "Preparation and Photovoltaic Evaluation of CuO@Zn(Al)O-Mixed Metal Oxides for Dye Sensitized Solar Cell," *Nanomaterials*, vol. 13, no. 5, p. 802, 2023, doi: 10.3390/nano13050802.
- [24] J.-P. Bäcker, "In situ investigation of the rapid thermal reaction of Cu-In-Ga precursors to Cu(In,Ga)Se₂ thin-film solar cell absorbers," 2018, doi: dx.doi.org/10.17169/refubium-293.
- [25] B. Lara-Lara and A. M. Fernández, "Growth improved of CIGS thin films by applying mechanical perturbations to the working electrode during the electrodeposition process," *Superlattices Microstruct.*, vol. 128, no. October 2018, pp. 144–150, 2019, doi: 10.1016/j.spmi.2019.01.024.
- [26] N. Mufti *et al.*, "Photoelectrochemical Performance of ZnO Nanorods Grown on Stainless Steel Substrate," *IOP Conf. Ser. Mater. Sci. Eng.*, vol. 515, no. 1, 2019, doi: 10.1088/1757-899X/515/1/012023.
- [27] G. Richhariya, A. Kumar, A. K. Shukla, K. N. Shukla, and I. Chanakaewsomboon, "Efficient photosensitive light harvesting dye sensitized solar cell using hibiscus and rhodamine dyes," *J. Power Sources*, vol. 572, p. 233112, 2023, doi: 10.1016/j.jpowsour.2023.233112.
- [28] Y. Zhao *et al.*, "Enhanced near-infrared photoresponse for efficient organic solar cells using hybrid plasmonic nanostructures," *Phys. E Low-Dimensional Syst. Nanostructures*, vol. 146, p. 115534, 2023, doi: 10.1016/j.physe.2022.115534.
- [29] S. Pandharkar *et al.*, "Enhanced photoresponse of Cu₂ZnSnS₄ absorber thin films fabricated using multi-metallic stacked nanolayers," *RSC Adv.*, vol. 13, no. 18, pp. 12123–12132, 2023, doi: 10.1039/d3ra00978e.